

LONGITUDINAL PHASE-SPACE AND TRANSVERSE SLICE EMITTANCE MEASUREMENTS OF HIGH-BRIGHTNESS ELECTRON BEAMS

R. Kato[#], S. Kashiwagi, Y. Morio, K. Furuhashi, Y. Terasawa, N. Sugimoto, G. Isoyama
 ISIR, Osaka University, Ibaraki, Osaka 567-0047, Japan

Abstract

In order to measure the longitudinal phase-space profile of the electron beam, we are developing a compact measurement system consisting of a Cherenkov radiator, a bending magnet and a streak camera. The Cherenkov radiator with an aerogel is installed in the beam transport line, and the electron distribution in the longitudinal phase-space is obtained. Furthermore, a slice emittance measurement system with the same method is proposed.

INTRODUCTION

The performance of the free-electron laser based on self-amplified spontaneous emission (SASE-FEL) strongly depends on time-sliced characteristics of the electron beam, such as longitudinal charge distribution, slice energy spread and transverse slice emittance. Recently, several methods are extensively under study to evaluate the longitudinal phase-space distribution of the electron beam [1-4] and the transverse slice emittances [5-7]. Among them, a streak camera system combined with Cherenkov radiation [2] or synchrotron radiation [4] was used to measure the electron distribution in the longitudinal phase-space.

A compact measurement system of the longitudinal phase-space distribution of electrons using the combination of a bending magnet, a Cherenkov profile monitor and a streak camera are currently under development at the Institute of Scientific and Industrial Research (ISIR), Osaka University [8-9]. Since the bending magnet produces momentum dispersion in the electron beam, electrons diverge in the horizontal direction. The Cherenkov radiator is placed on the beam transport line downstream from the bending magnet and it works as a converter from electrons to photons. In order to increase the number of photons, we try to use a Silica aerogel as a Cherenkov radiator using example from the results at PITZ [2]. The horizontal intensity distribution of photons is proportional to the momentum distribution of electrons, provided that the beam size of the electron beam due to the transverse emittance is negligibly small compared with the momentum distribution. By means of an appropriate optical system, the intensity distribution of photons on the Cherenkov radiator can be focused on the slit of the streak camera. When the temporal sweep of the camera is turned on, a streak image reproduces the electron distribution in the longitudinal phase-space.

In order to verify the idea, first longitudinal phase-space measurement was attempted with an optical transport system consisting of existing mirrors. Since the

optical transport system was not optimized, the energy acceptance was restricted to 1.1%. Therefore, we measured the energy sliced longitudinal phase-space images while changing the magnetic field of the bending magnet and reconstructed the preliminary longitudinal phase-space profile from the images [10]. After that, since the energy acceptance was expanded to 3% by improving the optical transport system, the longitudinal phase-space distribution has been measured as a single-shot image.

Moreover, it is easy to convert the longitudinal phase-space measurement system to the transverse slice emittance. Installing the Cherenkov radiator downstream of the quadruple magnet, we will be able to measure the time-resolved transverse beam sizes. Owing to scan the quadruple magnet field, the transverse slice emittances will be evaluated.

In this contribution, we will present preliminary experimental results of the longitudinal phase-space measurements and the plan of the transverse slice emittance measurement.

DESIGN OF CHERENKOV RADIATOR

Due to the physical limitation at the installation location, we could not bring a complicated mechanism into a vacuum. We designed a simple radiator supported with a metallic mirror as shown in Figure 1. In this radiator, we use a hydrophobic silica aerogel (SP-50, Panasonic Electric Works, Ltd.). A thin aerogel with a dimension of 45 x 30 mm² and a thickness of 1.5 mm is mounted on an aluminium metallic mirror. Refractive index and density of the aerogel are 1.05 and 0.19 g/cm³, respectively. Cherenkov radiation is emitted in a cone

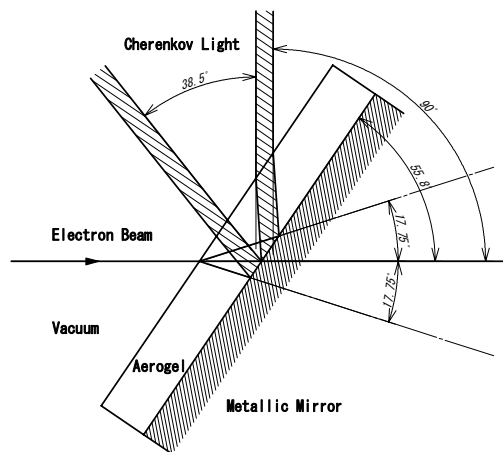


Figure 1: Schematic design of the Cherenkov radiator.

[#]kato@sanken.osaka-u.ac.jp

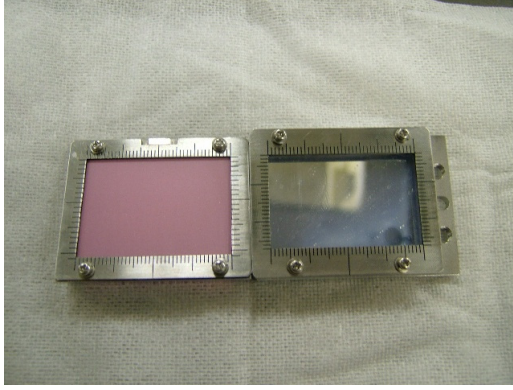


Figure 2: Screen folder mounted with both a ceramic screen and a Cherenkov radiator. The left screen is a profile monitor with a fluorescence ceramic screen with a thickness of 0.1 mm and it is tilted vertically by an angle of 45° . The right screen is the aerogel radiator and it is tilted of 55.8° .

having a subtended angle $2\theta_{CR}$, which is determined by the average index of refraction in the medium n and the particle velocity β as follows:

$$\cos \theta_{CR} = \frac{1}{\beta n}. \quad (1)$$

For electron energies above 10 MeV, the emission angle is almost constant and the subtended angle is 35.5° . Since the angle is too large to gather all rays of light, we use a part of the Cherenkov light. The light is reflected by the metallic mirror into the aerogel again, and is refracted by the surface between the aerogel and a vacuum. In order that the direction of the Cherenkov radiation emitted upward in the aerogel may be perpendicular to the horizontal plane in a vacuum, the radiator is attached with a tilt angle of 55.8° . Hereby the effective thickness of the aerogel becomes 2.7 mm. A part of the Cherenkov light cone is taken out from the vacuum chamber to the air through a sapphire vacuum window and is transported to the streak camera by mirrors. The light accepted by the first concave mirror is estimated approximately to 10% of the total radiation. The number of photons N_{CR} radiated in the wavelengths between λ_1 and λ_2 per a distance d along the path of the electrons is represented as follows:

$$N_{CR} = 2\pi\alpha d \left(\frac{1}{\lambda_1} - \frac{1}{\lambda_2} \right) \sin^2 \theta_{CR}, \quad (2)$$

where α is the fine structure constant. Assuming that the average transmittance of the aerogel is 85 % in the wavelength range from 400 nm to 800 nm, the photon yield on the first mirror is expected to 1.2 photons per incident electron.

Figure 2 shows the photograph of the screen folder mounted with the Cherenkov radiator. In order to measure the beam profile at the same location, a fluorescence ceramic screen (AF995R, Desmarquest) with a thickness of 0.1 mm is mounted next to the aerogel and its tilting angle is 45° with respect to the bending orbital plane.

FEL Technology I : Accelerator

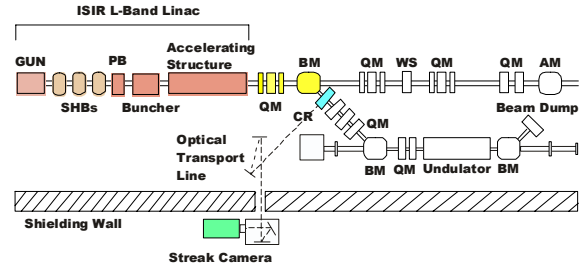


Figure 3: Schematic layout of the ISIR L-band Linac. The Cherenkov radiator was installed in the beam transport line from the linac to the FEL system.

LONGITUDINAL PHASE-SPACE MEASUREMENTS

The Cherenkov radiator was installed in the beam transport line from the linac to the FEL system as shown in Figure 3. The distance between the radiator and the bending magnet is 320 mm and the dispersion function η at this position is 0.4 m. Since the effective view width of the aerogel is 40 mm, the maximum energy acceptance and the energy resolution on the radiator are estimated to be 10% and 0.25% / mm, respectively.

The light generated by the aerogel in the linac room is carried in the atmosphere on the optical transport system of about 15 m, and measured with the streak camera in the measurement room. The streak camera converts an optical image on the input slit to a streak image with spatial information displayed on the horizontal axis and time on the vertical axis. We are using the streak camera C5680-11 (Hamamatsu Photonics), which has the temporal resolution of 1.57 ps with the fast speed sweep unit C5676. The effective area of the streak camera is $11(\text{H}) \times 8.25(\text{V}) \text{ mm}^2$. So we have to adjust the aerogel image into the area using an optical transport system.

The focal length of the first collimator mirror and the last focusing mirror in the optical transportation used this time are 500 mm and 250 mm, respectively. As a result, the horizontal size on the aerogel subtended from the streak camera is limited only to 22 mm, which is corresponding to the energy acceptance of 5.5% in the calculation. Both ends of the profile image were actually cut down while transporting it and the effective energy acceptance is limited to 3%. The effective energy resolution is decided by the square root of the product of the horizontal emittance and the beta function at the position of the Cherenkov screen. Though the slice emittance is needed to evaluate the energy resolution in the longitudinal phase-space correctly, it is estimated to be 0.3% using the projected emittance.

EXPERIMENTAL RESULTS

Figure 4 shows the energy spectrum of the single bunch electron beam which was used for the experiment. The electron bunch was accelerated by the 1.3 GHz L-band electron linac which has a three stage sub-harmonic

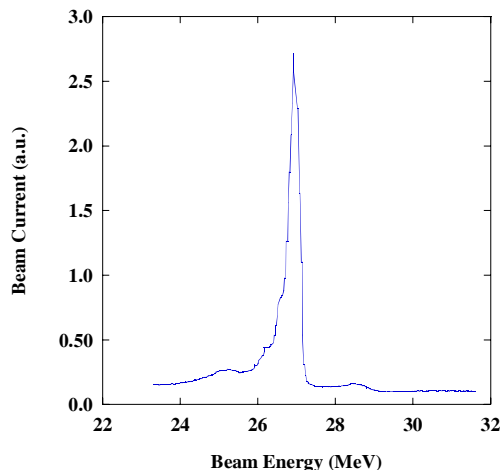


Figure 4: Energy spectrum of the single bunch electron beam with the peak energy of 26.9 MeV and the total charge of 30 nC.

buncher (SHB) system composed of two 108 MHz and one 216 MHz cavities. Due to the SHB system, it becomes possible to produce the high current electron bunch. Obtaining with a momentum analyser magnet, the peak energy is 26.9 MeV and the energy width (FWHM) is 1.3%. The charge of acceleration for each bunch is roughly presumed to be 30 nC.

Figure 5 shows the screen shot of the streak camera operation console. The streak image in the figure shows the longitudinal phase-space distribution when adjusted for an energy spectrum width to narrow most. The image

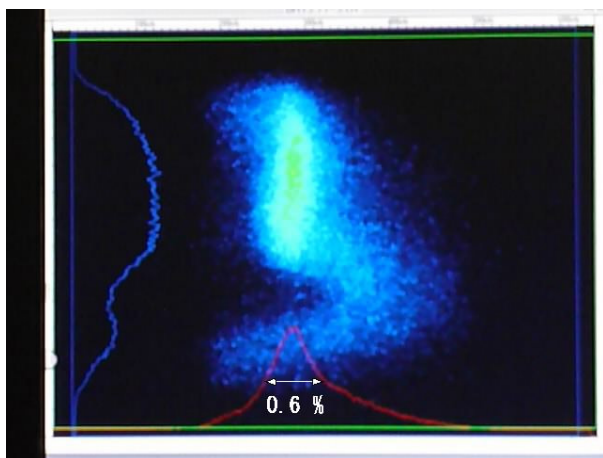


Figure 5: Longitudinal phase-space profile of the single bunch electron beam. The horizontal axis in the profile image shows beam energy and the vertical shows time (150 ps / full scale). The upper side indicates the head of the electron bunch and the right side the higher energy side.

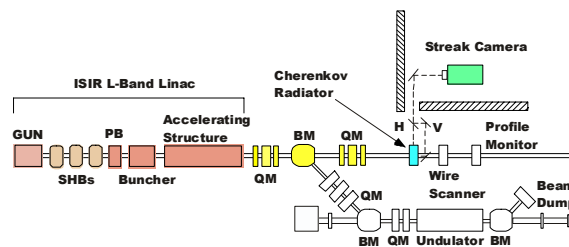


Figure 6: Schematic layout of the slice emittance measurement system. The Cherenkov radiator will be installed just downstream of the Q-magnets in the beam transport line.

in the figure has energy information as the horizontal axis and temporal one as the vertical axis. The upper part shows the head of the electron bunch and the right side the higher energy side. It can be understood that smooth flat energy part has been achieved in the distribution of electron bunch from the head to the center part. The flat part has been achieved by cancelling positive slope of an acceleration field by the external RF source and negative slope of the short-range wake-field generated in accelerating structure by the electron beam. In order to cancel the fields, the center of electron bunch is put on a phase forward from the crest of the acceleration field. Since the acceleration field is larger than the wake-filed in the tail of the bunch, the energy of the tail part rises.

The observed bunch length is approximately 60 ps, and it is longer than the typical length of 20-30 ps. This can be interpreted as the result of the adjustment for the wake-field to suppress the energy spread to lower. The energy spectrum and the temporal profile projected in each axis are shown in a red line and a blue line, respectively. The energy spectrum obtained from the phase-space distribution is 0.6% (FWHM), and it is narrower than the result of obtaining with the above-mentioned momentum analyser magnet. This result shows that the system has a high energy resolution rather than the momentum analyser system.

The temporal gap of the simultaneity at both ends of the image caused by the transfer matrix element of R_{56} is ± 3.7 ps and it is sufficiently small in this time scale.

TRANSVERSE SLICE EMITTANCE MEASUREMENTS

Up to now, the longitudinal phase-space measurement technique has been developed. This technique can be extended to the evaluation of the time-resolved beam sizes in the electron bunch by using quadruple magnet for the replacement of the bending magnet. By combining this with Q-scanning method, it becomes possible to measure the time-sliced transverse emittances. In order to verify this idea, the Cherenkov monitor with the aerogel is newly installed on the straight beam transport line of L-band linac as shown in Figure 6. Slice emittances of the electron beam are evaluated by sweeping the transverse

distribution of the electron beam with the streak camera while changing the focusing force of the quadruple magnet. In this technique, the system is simplified with the streak camera for the temporal sweep.

- [9] R. Kato et al, FEL'07, BINP, Novosibirsk, Russia, August 2007, p.409.
 [10] R. Kato et al, EPAC'08, Genoa, Italy, June 2008, p.1161.

SUMMARY

In order to measure the longitudinal phase-space profile of the electron beam, we are developing the measurement system consisting of the Cherenkov radiator, the bending magnet and the streak camera. The Cherenkov radiator with the aerogel was installed in the beam transport. We measured the preliminary longitudinal phase-space profile.

The temporal resolution of this system depends on the performance of the streak camera. If we use the fast streak camera, we can improve the resolution down to 200 fs. However, it is insufficient to use this as a monitor of a state-of-the-art accelerator that has the bunch length of 100 fs or less. On the other hand, the energy resolution is decided by the horizontal emittance and the beta function at the location of the Cherenkov radiator. The measurement system has higher energy resolution rather than the existing momentum analyser system.

This monitor system can be easily installed instead of the existing profile monitor since it is compact. Moreover, this technique can be easily extended to the transverse slice emittance measurements.

ACKNOWLEDGEMENTS

The authors express their sincere thanks to Mr. S. Suemine for his support of linac operation. This research is partially supported by Japan Society for the Promotion of Science (JSPS), Grant-in-Aid for Scientific Research (C), 18540273, 2006-2008 and Grant-in-Aid for Scientific Research (C), 21540298, 2009.

REFERENCES

- [1] A. Doria et al., Nucl. Instr. and Meth. in Phys. Res. A 475, (2001) 296.
 [2] J. Rönsch et al, FEL'06, BESSY, Berlin, Germany, August 2006, p.597.
 [3] H. Loos et al, FEL'05, Stanford, USA, August 2005, p.632.
 [4] S. Zhang et al, FEL'05, Stanford, USA, August 2005, p.640.
 [5] X. Qiu et al, Phys. Rev. Lett. 76, (1996) 3723.
 [6] D. H. Dowell et al, PAC'03, Portland, USA, May 2003, p. 2104.
 [7] M. Röhrs et al, EPAC'06, Edinburgh, Scotland, June 2006, p. 77.
 [8] R. Kato et al, FEL'06, BESSY, Berlin, Germany, August 2006, p.676.